

Observation of the optical $X^2\Sigma_g^+$-$A^2\Pi_u$ coupling in N_2^+ lasing induced by intense laser field

Siqi Wang(王思琪)[1], Yao Fu(付尧)[1], Danwen Yao(姚丹雯)[1], Shanming Chen(陈善铭)[1], Wei Zhang(张维)[1], Helong Li(李贺龙)[1,2], Huailiang Xu(徐淮良)[1,3]

Citation: Chin. Phys. B . 2019, 28(12): 123301 . **doi:** 10.1088/1674-1056/ab54b1
Journal homepage: http://cpb.iphy.ac.cn; http://iopscience.iop.org/cpb

What follows is a list of articles you may be interested in

Attosecond transient absorption spectroscopy: Comparative study based on three-level modeling

Zeng-Qiang Yang(杨增强), Di-Fa Ye(叶地发), Li-Bin Fu(傅立斌)

Chin. Phys. B . 2018, 27(1): 013301 . **doi:** 10.1088/1674-1056/27/1/013301

Frequency dependence of quantum path interference in non-collinear high-order harmonic generation

Shi-Yang Zhong(钟诗阳), Xin-Kui He(贺新奎), Hao Teng(滕浩), Peng Ye(叶蓬), Li-Feng Wang(汪礼锋), Peng He(何鹏), Zhi-Yi Wei(魏志义)

Chin. Phys. B . 2016, 25(2): 023301 . **doi:** 10.1088/1674-1056/25/2/023301

Quantum path control using attosecond pulse trains via UV-assisted resonance enhance ionization

Li Fang, Wei Lai, He Zhi-Cong

Chin. Phys. B . 2015, 24(4): 043301 . **doi:** 10.1088/1674-1056/24/4/043301

SPECIAL TOPIC — Strong-field atomic and molecular physics

Observation of the optical $X^2\Sigma_g^+$–$A^2\Pi_u$ coupling in N_2^+ lasing induced by intense laser field*

Siqi Wang(王思琪)[1], Yao Fu(付尧)[1], Danwen Yao(姚丹雯)[1], Shanming Chen(陈善铭)[1], Wei Zhang(张维)[1], Helong Li(李贺龙)[1,2,†], and Huailiang Xu(徐淮良)[1,3,‡]

[1] State Key Laboratory of Integrated Optoelectronics, College of Electronic Science and Engineering, Jilin University, Changchun 130012, China
[2] Institute of Atomic and Molecular Physics, Jilin University, Changchun 130012, China
[3] State Key Laboratory of Precision Spectroscopy, East China Normal University, Shanghai 200062, China

(Received 26 August 2019; revised manuscript received 12 October 2019; published online 29 November 2019)

We propose a simple pump-coupling-seed scheme to examine the optical $X^2\Sigma_g^+$–$A^2\Pi_u$ coupling in N_2^+ lasing. We produce the N_2^+ lasing at 391 nm, corresponding to the $B^2\Sigma_u^+(v'=0)$–$X^2\Sigma_g^+(v=0)$ transition, by externally seeding the N_2^+ gain medium prepared by irradiation of N_2 with an intense pump pulse. We then adopt a weak coupling pulse in between the pump and seed pulses, and show that the intensity of the 391-nm lasing can be efficiently modulated by varying the polarization direction of the coupling pulse with respect to that of the pump pulse. It is found that when the polarization directions of the pump and coupling pulses are perpendicular, the 391-nm lasing intensity is more sensitive to the coupling laser energy, which reflects the inherent nature of the perpendicular $X^2\Sigma_g^+$–$A^2\Pi_u$ transition.

Keywords: air lasing, intense laser fields, nitrogen molecules

PACS: 33.20.Xx **DOI:** 10.1088/1674-1056/ab54b1

1. Introduction

Nonlinear propagation of the powerful femtosecond laser pulses in the atmosphere induces many fascinating phenomena,[1–6] among which the so-called air lasing has attracted a lot of interests in recent years.[2–5] Air lasing is referred to remote mirrorless optical amplification in air with atmospheric constituents as the gain media,[7] and regarded as a promising tool in atmospheric applications for detection of, e.g., molecular rotational coherence[8] and stimulated Raman scattering.[9,10] So far, a variety of air lasing schemes with N_2, N_2^+, Ar, N, and O as the gain media have been developed,[11–18] in which the N_2^+ lasing on the $B^2\Sigma_u^+$–$X^2\Sigma_g^+$ transition has been intensively studied because of the mystery of its operation mechanism.[19–22] Since it was theoretically predicted that strong-field ionization of N_2 could not directly produce the population inversion between the $B^2\Sigma_u^+$ and $X^2\Sigma_g^+$ states in N_2^+,[23,24] several post-ionization scenarios have been proposed for interpretation of the N_2^+ lasing.[25–29]

Recently, it was reported that the intermediate state $A^2\Pi_u$ may play a key role in establishing the population inversion between the $B^2\Sigma_u^+$ and $X^2\Sigma_g^+$ states.[26,27] Through a post-ionization optical coupling process, the transfer of the population from $X^2\Sigma_g^+$ to $A^2\Pi_u$ takes place, which depletes the population in the $X^2\Sigma_g^+$ state, resulting in the population inversion between the $B^2\Sigma_u^+$ and $X^2\Sigma_g^+$ states.[26] It was further demonstrated with pump–probe methods that periodic oscillations of the intensity of the N_2^+ lasing at 391 nm can be achieved by finely scanning the time delay between the pump and probe pulses.[30,31] The Fourier transformation revealed that the oscillation periods correspond to the $X^2\Sigma_g^+(v=0)$–$A^2\Pi_u$ transition, which clearly showed the existence of the $X^2\Sigma_g^+$–$A^2\Pi_u$ coupling in the N_2^+ lasing process.

More recently, it was demonstrated that the intensity of N_2^+ lasing at 391 nm can be significantly enhanced with the pump of a polarization-modulated laser pulse, which was ascribed to more efficient population transfer from $X^2\Sigma_g^+$ to $A^2\Pi_u$ by the perpendicular component of the electronic field of the rear part of the laser pulse,[32] since the perpendicular $A^2\Pi_u$–$X^2\Sigma_g^+$ transition would strongly depend on the polarization direction of the coupling field. However, because of the complex polarization state modulation within the single pulse where the polarization state of the rear part of the laser pulse varies in time, it is not clear how the polarization state of the laser pulse contributes to the $X^2\Sigma_g^+$–$A^2\Pi_u$ coupling.

In the present study, we investigate the $X^2\Sigma_g^+(v=0)$–$A^2\Pi_u(v'=2)$ coupling effect in N_2^+ lasing by introducing a pump-coupling-probe scheme, in which an intense 800-nm pump light induces the ionization of nitrogen molecules, a

*Project supported by the National Natural Science Foundation of China (Grant Nos. 61625501, 11904121, and 61427816), the Open Fund of the State Key Laboratory of High Field Laser Physics (SIOM), China, the Program for JLU Science and Technology Innovative Research Team (JLUSTIRT), China (Grant No. 2017TD-21), and Fundamental Research Funds for the Central Universities of China.

†Corresponding author. E-mail: helongli@jlu.edu.cn
‡Corresponding author. E-mail: huailiang@jlu.edu.cn

© 2019 Chinese Physical Society and IOP Publishing Ltd

weak 800-nm laser pulse injected into the N_2^+ system about 70 fs after the pump laser functions with the coupling pulse to modulate the $X^2\Sigma_g^+(v=0)$ and $A^2\Pi_u(v'=2)$ coupling, and then a 400-nm broadband pulse is used to externally seed the N_2^+ gain medium. We observe that the intensity of the N_2^+ lasing at 391 nm first increases and then decreases as the angle θ between the polarization directions of the pump and coupling pulses increases from 0° to 180°. The intensity reaches the maximum at around $\theta = 90°$. In addition, it is found that when $\theta = 90°$, the lasing intensity increases linearly as the coupling laser energy increases, while when $\theta = 0°$, it keeps almost constant as the coupling laser energy increases. Our results suggest the resonant coupling between the $X^2\Sigma_g^+$ and $A^2\Pi_u$ states plays a key role in establishing the population inversion of N_2^+.

2. Experimental setup

Figure 1 shows the schematic diagram of the experimental setup for the pump-coupling-probe measurement. The experiments were conducted using a Ti: sapphire femtosecond laser system (Spectra Physics, Spitfire ACE), launching the laser pulses with a pulse duration of 40 fs, a central wavelength of 800 nm, an energy of up to 5 mJ, and a repetition frequency of 1 kHz. The laser beam was first divided by a 9 : 1 beam splitter into two arms. The weaker arm was used to generate a 400-nm second-harmonic laser by a 100-μm-thick barium borate (BBO) crystal as the external seed. The stronger one was further divided by a 6 : 4 beam splitter into two, which served as the pump and coupling, respectively. The coupling pulse energy was controlled by an 800-nm half-wave plate (HWP1) and a polarizer, and the polarization direction was varied by another half-wave plate (HWP2). The pump and coupling pulses were combined by a 5 : 5 beam splitter. After reflected by a dichroic mirror with high transmission at ∼ 400 nm and high reflectivity at ∼ 800 nm, the pump and coupling pulses were combined with the seed pulse by another dichroic mirror. The polarization direction of the seed pulse was adjusted by a 400-nm half-wave plate (HWP3) so that it was parallel to the horizontally polarized pump pulse. The time delay between the pump and coupling pulses and that of the pump and seed pulses were set to be 70 fs and 200 fs respectively by two delay lines with the resolution of 10 fs. When the polarization directions of the pump and the coupling pulses are parallel, the delay time of 70 fs can guarantee that the interference between the two 40-fs pulses is negligible. In addition, within this period of 70 fs, the molecular alignment of N_2^+ would not change so much.[33] The three sequential laser pulses were focused by a 40-cm fused silica lens into a N_2 chamber with a pressure of 10 mbar. The laser energies of the pump and seed pulses were set to be 700 μJ and 50 nJ, respectively.

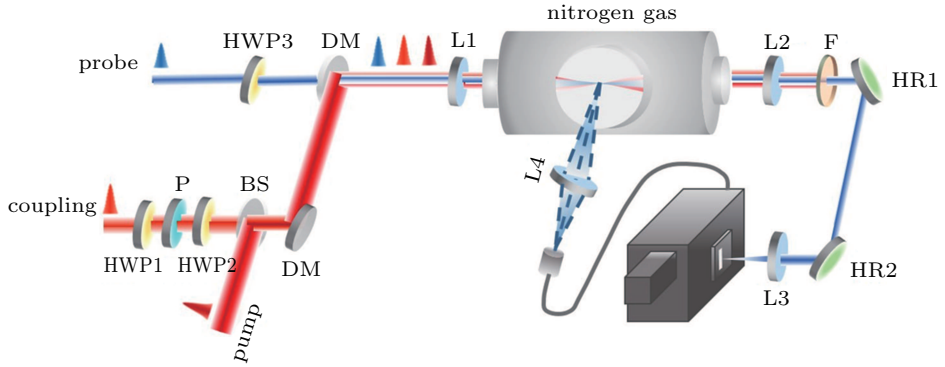


Fig. 1. Schematic of experimental setup based on the pump-coupling-probe scheme. HWP1 and HWP2: half-wave plate of 800-nm laser, HWP3: half-wave plate of 400-nm laser, P: polarizer, BS: beam splitter, DM: dichromic mirror, L1: fused silica lens with $f = 40$ cm, L2: fused silica lens with $f = 30$ cm, F: filter, HR1 and HR2: high reflection mirror of 400-nm laser, L3 and L4: fused silica lens with $f = 6$ cm.

After passing through the chamber, the laser pulses were collimated by a 30-cm fused silica lens. The 800-nm laser was removed by a filter with a high transmission at the UV range and the seed and the generated pulses were focused by a 6-cm fused silica lens onto the entrance slit of a 1200-grooves/mm grating spectrometer (Andor, Shamrock) coupled with an ICCD camera (Andor iStar). The slit width of the spectrometer was adjusted to be 150 μm. The gate delay and width of the ICCD were set at −5 ns (note the arrival time of the pump laser at the interaction zone is 0 ns) and 30 ns, respectively. The fluorescence emissions of N_2^+ were also collected by a 6-cm fused silica lens with a $2f$–$2f$ imaging scheme from the direction perpendicular to the laser propagation. The gate delay and width were set to 0 ns and 100 ns, respectively.

3. Results and discussion

Figure 2 shows the forward lasing spectra of N_2^+ in the spectral range of 388–393 nm, without (blue short dash) and with the coupling pulse whose polarization is arranged to be perpendicular (red solid) or parallel (pink dash) to that of the pump pulse, respectively. The signs ∥ and ⊥ represent the laser polarization direction parallel and perpendicular to the horizontal direction, respectively. The energy of the coupling

pulse was measured to be 180 μJ. The data were accumulated over 6000 laser shots. It can be seen that two strong lasing spectral bands around 389.5 nm and 391.4 nm appear, which are assigned to the R and P branches of the transition between the $B^2\Sigma_u^+(v'=0)$ and $X^2\Sigma_g^+(v=0)$ states of N_2^+. It should be emphasized that only with the pump pulse employed no lasing peaks appear in the forward spectrum in the spectral range of 388–393 nm. This is because the white-light spectrum resulting from the self-phase modulation effect cannot cover the 391 nm transition of N_2^+ due to the low laser energy of the pump pulse. It can be clearly observed from Fig. 2 that the coupling pulse triggers very different behaviors of the lasing emissions for the $B^2\Sigma_u^+(v'=0)$ and $X^2\Sigma_g^+(v=0)$ transition. That is, as the polarization direction of the coupling laser pulse is parallel to that of the pump pulse, the lasing intensity is comparable to that without the coupling, while as it is perpendicular to that of the pump, the lasing emission intensity is significantly enhanced by a factor of 5. It should be pointed out that when the polarization direction of the coupling pulse changes from parallel to perpendicular with respect to that of the pump pulse, an extra time delay (0.66 fs) between the pump and coupling pulses will be introduced by the rotation of HWP2. This extra delay may contribute to the modulation of the lasing signal, but it would be much smaller than what we have observed.[30]

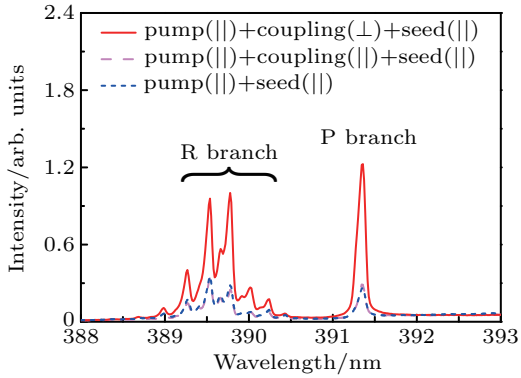


Fig. 2. Forward probe (seed) spectra when the pump laser is turned on without (blue short dash) and with the coupling laser whose polarization direction is parallel (pink dash) and perpendicular (red solid) to that of the pump. The signs ∥ and ⊥ represent the laser polarization direction parallel and perpendicular to the horizontal direction, respectively.

To further explore the influence of the polarization state of the coupling pulse on the lasing action of N_2^+, we measured the intensity of the forward lasing emission of N_2^+ at 391 nm as a function of the angle θ between the polarization directions of the pump and coupling pulses. The angle θ was controlled by rotating the 800-nm half-wave plate (HWP2 in Fig. 1) in the coupling arm. The energy of the coupling pulse before the lens was measured, and kept constant during the measurement by controlling the half-wave plate (HWP1) and the polarizer. The dependence of the 391-nm lasing intensity on the angle θ is presented in Fig. 3, where $\theta = 0°$ and 180° represent that the polarization directions of the coupling and pump pulses are parallel, and $\theta = 90°$ corresponds to the case that the polarization direction of the coupling pulse is perpendicular to that of the pump pulse. It can be seen from Fig. 3 that as θ increases from 0° to 180°, the lasing intensity first increases, and then decreases. The maximum is reached at about $\theta = 90°$. These results clearly demonstrate that the N_2^+ lasing is strongly dependent on the angle θ between the polarization directions of the pump and coupling pulses. It may be explained based on the coupling model presented in the inset of Fig. 3.[26] That is, at $\theta = 90°$, the coupling between the $A^2\Pi_u$ and $X^2\Sigma_g^+$ states is more efficient, leading to efficient population transfer from the $X^2\Sigma_g^+$ state to the population reservoir state $A^2\Pi_u$, and thus depleting the population in the $X^2\Sigma_g^+$ state.

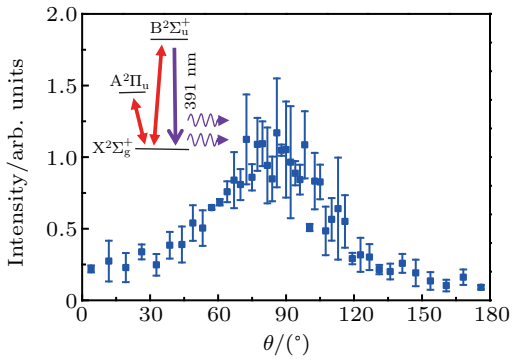


Fig. 3. Dependence of the 391-nm N_2^+ lasing intensity on the angle θ between the polarization directions of the coupling pulse and the pump pulse. Inset: schematic of post-ionization light-induced N_2^+ multiple-state coupling.

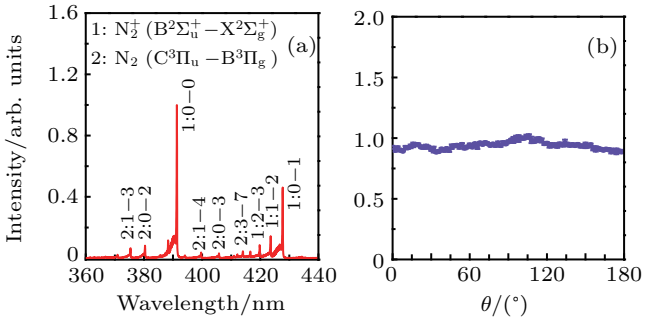


Fig. 4. (a) Typical fluorescence spectrum in pure N_2 gas induced by the laser field of the pump and coupling pulses obtained with $\theta = 90°$, (b) the intensity of the 391-nm fluorescence versus the angle θ between the polarization directions of the coupling pulse and the pump pulse.

It is also possible that the population in the $B^2\Sigma_u^+(v'=0)$ state is enhanced by the coupling field, leading to the increase of the population inversion between the $B^2\Sigma_u^+(v'=0)$ and $X^2\Sigma_g^+(v=0)$ states of N_2^+. In order to examine the variation of the population in the $B^2\Sigma_u^+(v'=0)$ state, we measured the fluorescence spectrum induced by the pump and coupling fields as a function of θ, from which we can analyze the population variation in the upper $B^2\Sigma_u^+(v'=0)$ level for the transition. Figure 4(a) shows a typical fluorescence spectrum obtained with $\theta = 90°$. In the measurements, the data were averaged over 4000 laser shots, and the probe laser was blocked. The

fluorescence spectral bands are assigned to the first negative band system of N_2^+ and the second positive band system of N_2. In Fig. 4(b), the intensity of the 391-nm fluorescence as a function of θ is plotted. It can be seen that the fluorescence emission intensity keeps almost constant as θ varies from 0° to 180°, indicating that the population in the $B^2\Sigma_u^+(v'=0)$ state is not sensitive to the coupling laser polarization direction. Therefore, it can be concluded that the significant increase in the N_2^+ lasing by the coupling field at $\theta = 90°$ mainly results from the population decrease on the $X^2\Sigma_g^+(v=0)$ state.

Next, we attempt to explain the polarization effect observed in Fig. 3 based on the post-ionization light-induced coupling model.[26,27] It is known that the N_2 molecules with the molecular axis parallel to the pump laser polarization are preferentially ionized.[34] Therefore, most of the N_2^+ ions are aligned along the pump laser polarization direction at the instant after the ionization. Under our current conditions, the temporal delay between the pump and the coupling pulses was set at 70 fs, within which the alignment of N_2^+ ions would not change so much.[33] Since the optical coupling between the $X^2\Sigma_g^+$ and $A^2\Pi_u$ states is achieved with perpendicular transition, as the laser polarization direction of the coupling pulse is perpendicular to that of the pump pulse, that is, the molecular axis of N_2^+, the coupling efficiency reaches the maximum, resulting in the significant enhancement of the population inversion between the $B^2\Sigma_u^+(v'=0)$ and $X^2\Sigma_g^+(v=0)$ states.

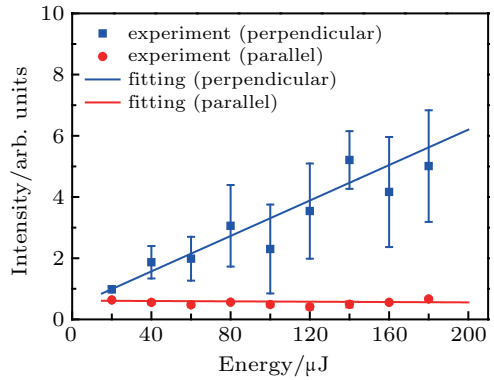


Fig. 5. Dependence of the 391-nm lasing intensity on the coupling laser energy with the polarization direction parallel (red circular) and perpendicular (blue square) to that of the pump.

On the other hand, the bandwidth of the pump pulse covers the transition $X^2\Sigma_g^+(v=0) \rightarrow A^2\Pi_u(v'=2)$,[30] and thus the $X^2\Sigma_g^+$–$A^2\Pi_u$ coupling is a resonant process with the pump of the 800 nm-wavelength laser. The coupling efficiency would be very sensitive to the input energy of the coupling pulse. To examine this, we measured the dependence of the 391 nm lasing intensity on the energy of the coupling laser with the polarization direction perpendicular and parallel to that of the pump, respectively. As shown in Fig. 5, it can be seen that as the input energy of the coupling pulse changes from 20 μJ to 180 μJ, the intensity of the 391-nm lasing shows totally different behaviors for the cases of $\theta = 0°$ and $\theta = 90°$. At $\theta = 90°$, the intensity of the 391-nm lasing linearly increases as the laser energy increases, while at $\theta = 0°$, the 391-nm lasing intensity keeps almost constant, both of which can be fitted well by a linear function (solid lines). This observation clearly indicates the strong dependence of the perpendicular $X^2\Sigma_g^+$–$A^2\Pi_u$ transition on the polarization state of the coupling field. It should be pointed out that the coupling efficiency would also be affected by the pump laser energy that determines the population distribution among the $X^2\Sigma_g^+$, $A^2\Pi_u$, and $B^2\Sigma_u^+$ states of N_2^+, which is however beyond the scope of this study.

4. Summary

We have investigated the resonant coupling effect on the perpendicular transition between the $X^2\Sigma_g^+$ and $A^2\Pi_u$ states in N_2^+ lasing by varying the polarization direction of the coupling pulse with respect to that of the pump pulse. We have demonstrated that the population transfer process from the state $X^2\Sigma_g^+(v=0)$ to the state $A^2\Pi_u(v'=2)$ is strongly influenced by the angle θ between the polarization directions of the coupling and the pump pulses, leading to intense modulation of the lasing intensity at 391 nm from the $B^2\Sigma_u^+(v'=0)$–$X^2\Sigma_g^+(v=0)$ transition. We have further showed that the 391-nm lasing intensity is more sensitive to the coupling laser energy at $\theta = 90°$, indicating the intrinsic nature of the perpendicular $X^2\Sigma_g^+$–$A^2\Pi_u$ transition. Our results further confirm that the light-induced resonant coupling between the $X^2\Sigma_g^+$ and $A^2\Pi_u$ states plays a key role in establishing the population inversion of N_2^+.

References

[1] Couairon A and Mysyrowicz A 2007 *Phys. Rep.* **441** 47
[2] Xu H L, Cheng Y, Chin S L and Sun H B 2015 *Laser Photon. Rev.* **9** 275
[3] Yuan S, Chin S L and Zeng H P 2015 *Chin. Phys. B* **24** 014208
[4] Chin S L and Xu H L 2015 *Chin. Phys. B* **24** 013301
[5] Chin S L and Xu H L 2016 *J. Phys. B: At. Mol. Opt. Phys.* **49** 222003
[6] Wolf J P 2017 *Rep. Prog. Phys* **81** 026001
[7] Li H L, Yao D W, Wang S Q, Fu Y and Xu H L 2019 *Chin. Phys. B* **28** 114204
[8] Zhang H, Jing C, Yao J, Li G, Zeng B, Chu W, Ni J, Xie H, Xu H, Chin S, Yamanouchi K, Cheng Y and Xu Z 2013 *Phys. Rev. X* **3** 041009
[9] Ni J, Chu W, Zhang H, Zeng B, Yao J, Qiao L, Li G, Jing C R, Xie H Q, Xu H, Cheng Y and Xu Z 2014 *Opt. Lett.* **39** 2250
[10] Malevich P N, Maurer R, Kartashov D, Ališauskas S, Lanin A A, Zheltikov A M, Marangoni M, Cerullo G, Baltuška A and Pugžlys A 2015 *Opt. Lett.* **40** 2469
[11] Luo Q, Liu W and Chin S L 2003 *Appl. Phys. B* **76** 337
[12] Dogariu A, Michael J B, Scully M O and Miles R B 2011 *Science* **331** 442
[13] Laurain A, Scheller M and Polynkin P 2014 *Phys. Rev. Lett.* **113** 253901
[14] Dogariu A and Miles R B 2016 *Opt. Express* **24** A544
[15] Mitryukovskiy S, Liu Y, Ding P J, Houard A and Mysyrowicz A 2014 *Opt. Express* **22** 12750

[16] Kartashov D, Ališauskas S, Andriukaitis G, Pugžlys A, Shneider M, Zheltikov A, Chin S L, Baltuška and A 2012 *Phys. Rev. A* **86** 033831
[17] Yao J, Zeng B, Xu H, Li G, Chu W, Ni J, Zhang H, Chin S L, Cheng Y and Xu Z 2011 *Phys. Rev. A* **84** 051802
[18] Xu B, Yao J P, Wan Y X, Chen J M, Liu Z X, Zhang F B, Chu W and Cheng Y 2019 *Opt. Express* **27** 18262
[19] Yao J, Li G, Jing C, Zeng B, Chu W, Ni J, Zhang H, Xie H, Zhang C, Li H, Xu H, Chin S L, Cheng Y and Xu Z 2013 *New J. Phys.* **15** 023046
[20] Wang T J, Daigle J F, Ju J, Yuan S, Li R and Chin S L 2013 *Phys. Rev. A* **88** 053429
[21] Point G, Liu Y, Brelet Y, Mitryukovskiy S, Ding P, Houard A and Mysyrowicz A 2014 *Opt. Lett.* **39** 1725
[22] Li H, Zang H, Su Y, Fu Y and Xu H 2017 *J. Opt.* **19** 124006
[23] Lofthus A and Krupenie P H 1977 *J. Phys. Chem. Ref. Data* **6** 113
[24] Zhao S F, Jin C, Le A T, Jiang T F and Lin C D 2010 *Phys. Rev. A* **81** 033423
[25] Liu Y, Ding P, Lambert G, Houard A, Tikhonchuk V and Mysyrowicz A 2015 *Phys. Rev. Lett.* **115** 133203
[26] Xu H, Lötstedt E, Iwasaki A and Yamanouchi K 2015 *Nat. Commun.* **6** 8347
[27] Yao J, Jiang S, Chu W, Zeng B, Wu C, Lu R, Li Z, Xie H, Li G, Yu C, Wang Z, Jiang H, Gong Q and Cheng Y 2016 *Phys. Rev. Lett.* **116** 143007
[28] Azarm A, Corkum P and Polynkin P 2017 *Phys. Rev. A* **96** 051401
[29] Yao J P, Chu W, Liu Z X, Chen J M, Xu B and Cheng Y 2018 *Appl. Phys. B* **124** 73
[30] Zhang A, Lei M, Gao J, Wu C, Gong Q and Jiang H 2019 *Opt. Express* **27** 14922
[31] Ando T, Lötstedt E, Iwasaki A, Li H, Fu Y, Wang S, Xu H L and Yamanouchi K 2019 *Phys. Rev. Lett.* **123** 203201
[32] Li H L, Hou M Y, Zang H W, Fu Y, Lötstedt E, Ando T, Iwasaki A, Yamanouchi K and Xu H L 2019 *Phys. Rev. Lett.* **122** 013202
[33] Litvinyuk I V, Lee K F, Dooley P W, Rayner D M, Villeneuve D M and Corkum P B 2003 *Phys. Rev. Lett.* **90** 233003
[34] Pavicić D, Lee K F, Rayner D M, Corkum P B and Villeneuve D M 2007 *Phys. Rev. Lett.* **98** 243001